An anti-liver tumor ingredient of Elephantopus tomentosus Linn. and the mechanism prediction by combining UPLC-Q-TOF-MS/MS, network pharmacology analysis and validating on HepG2

JIA Canchao
School of the fifth Clinical Medicine, Guangzhou University of Chinese Medicine
ZENG Zhihao
School of the fifth Clinical Medicine, Guangzhou University of Chinese Medicine
LI Lingjie
Guangzhou University of Chinese Medicine
JIA Dezheng
School of the fifth Clinical Medicine, Guangzhou University of Chinese Medicine
Ruiyin TANG
School of the fifth Clinical Medicine, Guangzhou University of Chinese Medicine
Yangxue LI
Guangdong Province Engineering Technology Research Institute of Traditional Chinese Medicine
XIAO Guanlin
Guangdong Province Engineering Technology Research Institute of Traditional Chinese Medicine
JIANG Jieyi
Guangdong Province Engineering Technology Research Institute of Traditional Chinese Medicine
Dake CAI
Department of Pharmacy, Guangdong Provincial People's Hospital, Guangdong Academy of Medical Sciences
Xiaoli Bi (zyfxyjs@gzucm.edu.cn)
Guangdong Province Engineering Technology Research Institute of Traditional Chinese Medicine

Article

Keywords: Elephantopus tomentosus Linn., UPLC-Q-TOF-MS/MS, Network pharmacology, Anti-tumor activity, HepG2, ST

Posted Date: January 3rd, 2024

DOI: https://doi.org/10.21203/rs.3.rs-3786326/v1

Additional Declarations: No competing interests reported.

Abstract

Elephantopus tomentosus (ET) Linn. was reported to be an anti-tumor plant. However, the chemical composition of ET and its anti-tumor compounds and potential mechanisms still unclear. In this paper, UPLC-Q-TOF-MS/MS was first used to identified the ingredients in ET and UPLC was used to determine the main compounds of ET. Network pharmacology was applied to predict the potential mechanisms. Anti-tumor nuclear activate compounds and targets of ET were obtained and the anti-liver cancer effect was validated on HepG2. Finally, Molecule docking, RT-qPCR, and western blotting were used for verification of the relationship between nuclear activate compounds and nuclear targets and the potential anti-cancer mechanisms. The result showed that 42 compounds were identified in ET, which consisted of sesquiterpene lactones, flavonoids, and phenylpropanoid compounds. Scabertopin (ST), chlorogenic acid, Isochlorogenic acid B, Isochlorogenic acid A and Isochlorogenic acid C were identified as main compounds and were determined as 0.426% 0.457% 0.159% 0.701%, and 0.103% respectively. 24 compounds of them show high pharmacokinetics and good drug-likeness. 520 targets were collected by searching on TCMSP, HIT, and Swiss Target Prediction. The targets were used for KEGG and GO analysis. GO enrichment analysis suggested that the targets of 24 active compound closed related to promote apoptosis, inhibit proliferation, and regulate oxidative levels. KEGG enrichment analysis suggested that pathway in cancer was enriched most and p38 MAPK/p53 signaling pathway, which closely related to promoting apoptosis and inhibiting proliferation, were obtained. Compounds-targets analysis based on the parameter of Betweenness, Closeness, Information, Eigenvector, Degree, and component content indicated that ST was the nucleus anti-tumor active compound of ET. HepG2 was first used to validated the anti-tumor effect of ST and the result showed that ST significantly inhibited HepG2 proliferation with a low IC50 less than 5 μM. Nucleus active compound targets, including TP53, CASP3, BCL2, EGFR, TNF-a, IL-1β, and IL-6 were enriched based on degree value of PPI analysis. Molecule docking suggested that ST showed a good combination to TGFBR1 with the combination energy less than − 5 kcal/mol. RT-qPCR result also suggested that ST significantly medicated the mRNA expression level of TP53, CASP3, BCL2, EGFR, TNF-a, IL-1β, and IL-6. Protein expression of p-p38/p38 and p-p53/p53 notable increased by ST treatment. In conclude, combining with UPLC-Q-TOF-MS/MS qualitative analysis, UPLC quantitative analysis, network pharmacology analysis, molecule docking, and in vitro experiments on HepG2, we suggest that ST is an anti-tumor ingredient of ET, which may target to TGFBR1 and promote apoptosis and inhibited proliferation of HepG2 by activating p38 MAPK/p53 signaling pathway. ST can be regarded as a quality marker of ET.

Introduction

Liver cancer is the sixth most malignancy all over the world and people die of liver cancer is second only to lung cancer. More seriously, incidence rate of liver cancer is getting higher and higher and it will be a societal burden and bring great health challenge to human beings [1]. Interaction between liver metabolic disease, such as obesity, fatty liver, and cirrhosis, and liver cancer make the treatment of liver cancer more complex [2]. Meanwhile, inflammatory responses, anomalies in the cell cycle, and immune dysfunction

may cause liver cancer singly or in combination [3]. Current drugs were not satisfactory for liver cancer patients suffering from complex conditions and diverse etiologies disease. Therefore, exploring alternative treatment drugs and methods is still urgent.

Traditional Chinese medicine (TCM) played an important role in combating liver cancer and has attracted more and more attention all over the world. Traditional Chinese medicine adopts a dialectical approach to treatment, which highlights better therapeutic effects in the face of complex diseases. In addition, TCM attenuated toxic and side effects of chemotherapy and radiotherapy. Therefore, TCM was widely used in clinical practice [4,5]. Therefore, exploring anti-liver cancer drugs from TCM show a widely prospect.

Elephantopus tomentosus L. (Asteraceae) is a traditional medicine widely used to treat cold, hepatitis, bronchitis, fever, the cough associated with pneumonia, and arthralgia in south of China, Hong Kong, Macao and Taiwan areas [6]. Since 1970s, American and Japanese scholars have successively discovered sesquiterpene lactones compounds from ET, which show obvious anti-tumor activity [7,8]. In recent years, more and more scholars played attention to ET and different kinds of compounds of ET has been found and identified and most of the compounds showed significant anti-cancer effect [9]. Therefore, in this study, the chemical components of ET were analyzed by UPLC-Q-TOF-MS/MS and the main compounds' content was determined. Network pharmacology was applied to predict the potential mechanisms, nuclear activate compounds and targets of ET and validated on HepG2. Finally, Molecule docking and RT-qPCR were used for verification of the relationship between compounds and targets and the potential anti-cancer mechanisms. Our aim was to explore chemical composition of ET and its anti-liver cancer compounds and potential mechanisms, which finally provide alternative treatment options for liver cancer.

Materials and Methods

2.1 Materials

Methanol, formic acid, and acetonitrile of MS grade were purchased from Thermo Fisher Scientific (Thermo, United States). Laboratory-deionized water was generated by a Milli-Q water purification system (Millipore, United States). The fresh whole plants of ET were contributed by Zhan Lu of the Medicinal Botanical Garden of Guangzhou University of Chinese Medicine (Guangzhou, China) in September 2022 and were identified as *Elephantopus tomentosus* Linn. by Professors Fajin Liu (Guangdong Provincial Engineering Technology Research Institute of Traditional Chinese Medicine, Guangdong, China). ET samples were dried at 45 ◦C until reaching a constant weight and the voucher specimen (No. ET2022091001) was deposited at Guangdong Province Engineering Technology Research Institute of Traditional Chinese Medicine, Guangzhou, China. The dried ET was grinded into fine powder and stored at -20 ◦C before analysis. Primary anti-BCL-2, anti-CASP3, anti-p38, anti-p-p38 anti-p53, and anti-p-p53 were purchased from HuaBio (Hangzhou, China).

2.2 The preparation of ET sample solution and standard solution

1.0 g ET powder was accurately weighed and placed into a 150 flat-bottomed conical flask and immersed in 20 mL 70% methanol water. Then, ultrasound extraction was performed for 30 min. Last, ET sample was obtained by filtrating through a 0.22 μm filter membrane. All the standards (≥ 95% purity, HPLC), including, Chlorogenic acid, Sochlorogenic acid A, Isochlorogenic acid B, Isochlorogenic acid C, and ST were purchased from Chengdu Herbpurify Co., Ltd (Chengdu, China). The standards were weighted and dissolved in methanol (MS grade) for being analyzed.

2.3 UPLC-Q-TOF-MS/MS analysis conditions

Liquid chromatography analysis was performed on a SHIMADZU Exion LC system (Japan) with an Acquity BEH C18 column (100 × 2.1 mm, 1.7μm, Waters, MA, USA) and the mobile phase consisted of 0.1% formic acid aqueous solution (A) and methanol (B) : 0 3min, 5 20% B;3 7 min, 20% 45% B 7 12min, 45% 55% B, 12 20min, 55% 70% B, 20 25min, 70% 88% B, 25 27min, 88% 100% B. The flow rate was 0.25 mL/min with the column temperature fixed at 40 ℃ and the injection volume was 1.0 μL.

The MS analysis was conducted by using an AB SCIEX X500R Q-TOF-MS/MS system (United States) with an electrospray ionization (ESI). The instrumental settings of Q-TOF-MS/MS were as follows: ion source gas 1 and gas 2 were both 50 psi, curtain gas was 35 psi, ion source temperature was 500 ℃, an ion-spray voltage of + 5500/ -4500 V, a declustering potential voltage of 100/-80 V and a collision energy of ± 35 V, collision energy spread was 15 V. ET Samples were analyzed in both negative and positive ionization modes with scanning mass-to-charge (m/z) range from 100 to 1500. Data was collected in information-dependent acquisition (IDA) mode.

2.4 UPLC analysis conditions

UPLC analysis was carried out on a UPLC (2695, Waters, Ameircan), connecting with a CORTECS UPLC C18 column (2.1×150mm,1.6μm, Waters, Ameircan). The mobile phase consisted of acetonitrile (B) and 0.1 formic acid aqueous solvent (D) as follows: 0 5min, 10 15% B;5 10 min, 15% 20% B 10 15min, 20% 25% B, 15 20min, 25% 35% B, 20 25min, 35% 95% B, 25 30min, 95% 95% B 30 35min, 10% 10% B. The flow rate was 0.20 mL/min and the volume temperature fixed at 30°C. The injection volume was 1.0 μL and the detection wavelength was set at 240 nm.

2.5 Network Pharmacology

Compounds identified with Pharmacokinetic properties Gatrointestinal absorption as High, and two of druglikeness (Lipinski filter, Ghose filter, Veber filter, Egan filter, and Muegge filter) as high in SwissADME (http://www.swissadme.ch/) or OB ≥ 30% and DL ≥ 0.18 in TCMSP (https://tcmsp-e.com/tcmsp.php) were saved as active ingredients. The active ingredients were submitted to TCMSP (https://tcmsp-e.com/tcmsp.php), HIT (http://www.badd-cao.net:2345/textmining), and SwissTargetPrediction (http://www.swisstargetprediction.ch/, the parameter of probability ≥ 0.10) to figured out the potential

targets of ET. Liver cancer potential targets were collected from DisGeNET (https://www.disgenet.org/) database with the Score_gda ≥ 0.10, GeneCards (https://www.genecards.org/) database with relevance score ≥ 10.00, and OMIM (https://omim.org/) database and the union target was obtained for further study. The hub target of compound targets and disease targets was figure out by Venny 2.1.0 (https://bioinfogp.cnb.csic.es/tools/venny/) analysis. Hub targets were input to Cytoscape3.7.0 [10] to conduct compound-targets network and submitted to STRING (https://cn.string-db.org/) to create a protein-protein interaction (PPI) network. Hub targets were used for Kyto Encyclopedia of Genes and Genomes (KEGG) pathway enrichment and construct Gene Ontology (GO) biological functions enrichment analysis on metascape (https://metascape.org/gp/) database with the conditions of p value less than 0.01, minimum count as 3, and enrichment factor > 1.5.

2.6 Nuclear ingredients and targets Analysis

The overlapping compounds based on top 20 of Betweenness, Closeness, Information, Eigenvector, and Degree in compound-targets network and component content were regarded as nucleus active compound. Meanwhile, nucleus targets based on top 20 of Betweenness, Closeness, Information, Eigenvector, Degree, and Network in PPI network and Compound-targets network were figured out by vene analysis (https://www.bioinformatics.com.cn/).

2.7 Molecular Docking Analysis

The mol2 or PDB structure format files of the nuclear compounds were downloaded respectively from TCMSP (https://tcmsp-e.com/tcmsp.php) or PubChem (https://pubchem.ncbi.nlm.nih.gov/) database. PDB structure format files of the nuclear compounds were changed into mol2 structure format files by OpenBabel-3.1.1 (http://openbabel.org/). Mol2 structure format files of nuclear compounds were then input into AutoDock version 4.2 to add hydrogens, set as ligand, detect root, choose torsions, and save as “pdbqt” files. Meanwhile, PDB files of nuclear targets were downloaded from PDB database (https://www.rcsb.org/) and submitted to AutoDock version 4.2 to delete water, add hydrogens, choose as target, and save as “pdbqt” files. Nuclear compound and target in “pdbqt” files were input into AutoDock version 4.2 and a suitable grid box was set and then saved as “gpf” files. The “gpf” files was open in AutoDock version 4.2 and carried out “run autodrid”. After setting relevant parameter of docking, a “dpf” files was saved and finally carried out autodock running. 50 conformations were conducted in receptor–ligand interaction generation, and the best affinity was chosen as the final docking conformation and the binding energy ≤ − 5 kCal/mol was regarded as stable.

2.8 HepG2 Cell Culture and administrate

HepG2 cells were bought from National Collection of Authenticated Cell Culteres (China, Beijing) and cultured in MEM containing 10% fetal bovine serum (FBS, TransGen Biotech, China, Shanghai), 100 kU/L penicillin, and 100 mg/L streptomycin (TransGen Biotech, China, Shanghai) at 37°C in a 5% CO2 humidified incubator. When HepG2 cells were in good condition, ST (5 μM) was added to the cell and incubated for 24 hours.

2.8 HepG2 Cell proliferation detection

HepG2 cells were seeded into 96-well plates at a density of 5000 cells/well. The effect of ST on cell viability was analyzed after treatment for 24 h at different concentration of 0, 1.25, 2.5, 5, 10, and 20 μM. After treatment, 5% CCK8 (Solarbio, China, Beijing)/complete medium was added to the well and incubated for 1 hours. Absorbance was measured at 490 nm using a microplate reader (Thermo scientific, United States) and proliferation inhibit ratio was calculated.

2.9 Quantitative Real-Time PCR Analysis

Total RNA was extracted from HepG2 cells using Trizol reagent (Thermo Fisher Scientific, United States). 0.5 μg total RNA was reverse transcribed into cDNA with the Evo M-MLV RT Premix for qPCR (Accurate Biology, China) kit. DNA amplification was conducted by using PerfectStayt Green qPCR SuperMix (TransGen Biotech, China) on a StepOnePlus Real-Time PCR system (Thermo Fisher Scientific, United States). The primers sequences of nuclear genes were shown in Table 1. Relative mRNA levels were calculated by using $2^{-\Delta\Delta ct}$ method and visualized by Graphpad Prism 7.0.

Table 1
The primers sequences of nuclear genes

Name	F	R
TNF-α	GCTGCACTTTGGAGTGATCG	ATGAGGTACAGGCCCTCTGA
IL-1β	TACCTGTCCTGCGTGTTGAAA	GGTGCTGATGTACCAGTTGGG
IL-6	ATGAGGAGACTTGCCTGGTGAA	CTCTGGCTTGTTCCTCACTACTCTC
TGF-β1	CCCACAACGAAATCTATGACAAG	GCTGAGGTATCGCCAGGAAT
CASP3	TGGAAGCGAATCAATGGACTCT	TGAATGTTTCCCTGAGGTTTGC
BCL2	GGAGGATTGTGGCCTTCTTTG	GCATCCCAGCCTCCGTTATC
GAPDH	GGAAGCTTGTCATCAATGGAAATC	TGATGACCCTTTTGGCTCCC

2.10 Western blotting analysis

HepG2 co-cultivated with ST were lysed by RIPA Buffer (Sigma, USA) and centrifuged with the condition of 4 ℃, 12000 rpm and 10 min. The protein content was measured using Pierce BCA Protein Assay Kit (Thermo, USA) and diluted with loading buffer (Beibokit, China) to 5μg/μL. Protein in an equal amount were separated using SDS-polyacrylamide gel electrophoresis and transferred onto PVDF membranes (Bio-Rad, United States). PVDF membranes were blocked with 5% skim milk and then washed by TBST (0.5% Tween-50), and incubated with various primary antibody at 4 ℃ overnight. Primary antibody was recovered and the membranes were incubated with anti-rabbit horseradish peroxidase-conjugated secondary antibody (1:10000 dilution, Abcam). After washing three times, the membranes were enhanced by chemiluminescence in the ECL reagents (Thermo Fisher Scientific, United States). The membranes

were performed with the gel imaging analysis system (Tanon 5220 multi, China) and the image was acquired by Tanon Gis (Tanon 5220 multi, China). The gray value was determined with Image J software and visualized by Graphpad Prism 7.0.

2.11 Statistical analysis

All experiments were performed independently at least three times and the results were recorded as the mean ± SEM. A one-way ANOVA in SPSS 20.0 software was used to analyze the means between different groups. Differences were considered statistically significant when $p < 0.05$ in this study.

Results

3.1 Ingredient Analysis and Identification

The total ion chromatography (TIC) of ET in positive and negative ion modes was shown in Fig. 1. A total of 42 chemical constituents (shown in Table 2) were identified in ET by comparing to the reference standard, chromatographic elution behaviors, mass fragment patterns, and mass spectral data in Pubchem (https://pubchem.ncbi.nlm.nih.gov/), Scifinder (https://sso.cas.org/), and CNKI (https://www.cnki.net/).

Table 2
Chemical constituents of ET

NO.	Adduct / Charge	Component Name	Retention Time	Formula	Found At Mass	Mass Error (ppm)
1	[M-H]-	Quinic acid	1.166	C7H12O6	191.0559	-1.1
2	[M-H]-	L-Malic acid	1.310	C4H6O5	133.0140	-1.6
3	[M-H]-	Maleic acid	1.311	C4H4O4	115.0039	1.5
4	[M + H]+	Piceatannol	1.737	C14H12O4	245.0774	-14.0
5	[M-H]-	2-Hydroxyadenosine	2.314	C10H13N5O5	282.0856	4.2
6	[M-H]-	Guanosine	2.314	C10H13N5O5	282.0856	4.2
7	[M-H]-	Protocatechuic acid	3.675	C7H6O4	153.0200	4.4
8	[M-H]-	Neochlorogenic acid	4.052	C16H18O9	353.0874	-1.1
9	[M + H]+	Daphnetin	4.584	C9H6O4	179.0345	3.2
10	[M-H]-	Protocatechuic Aldehyde	4.600	C7H6O3	137.0246	1.3
11	[M-H]-	Chlorogenic acid	5.326	C16H18O9	353.0872	-1.7
12	[M-H]-	Esculetin	5.583	C9H6O4	177.0195	0.9
13	[M-H]-	Cryptochlorogenic acid	5.589	C16H18O9	353.0873	-1.5
14	[M + H]+	7-Hydroxycoumarine	5.593	C9H6O3	163.0389	-0.3
15	[M-H]-	Caffeic acid	5.834	C9H8O4	179.0351	0.9
16	[M-H]-	Schaftoside	7.196	C26H28O14	563.1406	0.0
17	[M-H]-	Isochlorogenic acid B	7.684	C25H24O12	515.1186	-1.8
18	[M-H]-	Isochlorogenic acid A	7.970	C25H24O12	515.1186	-1.8
19	[M + H]+	Aempferol-3-O-rutinoside	8.089	C27H30O15	595.1655	-0.5
20	[M-H]-	Luteolin-7-O-β-D-glucuronide	8.121	C21H18O12	461.0728	0.6
21	[M-H]-	(-)-Syringaresinol 4-O-β-D-glucopyranoside	8.245	C28H36O13	579.2086	2.4
22	[M-H]-	Isoquercitrin	8.316	C21H20O12	463.0886	3.2
23	[M-H]-	Isochlorogenic acid C	8.685	C25H24O12	515.1186	-1.8
24	[M-H]-	Ferulic acid	8.722	C10H10O4	193.0514	9.8
25	[M + H]+	Rhoifolin	8.731	C27H30O14	579.1726	3.0

NO.	Adduct / Charge	Component Name	Retention Time	Formula	Found At Mass	Mass Error (ppm)
26	[M-H]-	Apigenin 7-O-beta-D-glucuronide	8.843	C21H18O11	445.0778	0.3
27	[M + H]+	Sophoricoside	8.848	C21H20O10	433.1143	3.3
28	[M-H]-	Cosmosiin	8.850	C21H20O10	431.0995	2.7
29	[M-H]-	Luteoloside	9.050	C21H20O11	447.0934	0.2
30	[M + H]+	Elephantopin	9.291	C19H20O7	361.1291	2.4
31	[M-H]-	Apigenin	9.967	C15H10O5	269.0463	2.8
32	[M + H]+	Deoxyelephantopin	10.310	C19H20O6	345.1343	2.9
33	[M + H]+	Quercetin	10.424	C15H10O7	303.0504	1.5
34	[M-H]-	Molephantin	10.621	C19H22O6	345.2259	8.2
35	[M + H]+	Isodeoxyelephantopin	10.658	C19H20O6	345.1339	1.7
36	[M-H]-	Luteolin	10.960	C15H10O6	285.0399	-2.0
37	[M-H]-	Molephantinin	11.909	C20H24O6	359.1513	6.8
38	[M + H]+	ST	11.942	C20H22O6	359.1495	1.5
39	[M + H]+	IsoST	12.441	C20H22O6	359.1499	2.6
40	[M-H]-	Tricin	12.590	C17H14O7	329.0675	5.7
41	[M-H]-	Diosmetin	12.654	C16H12O6	299.0569	2.7
42	[M + H]+	Linderane	15.030	C15H16O4	261.1127	2.1

3.2 Quantification of 5 compounds in AT by UPLC

ST, chlorogenic acid, Isochlorogenic acid B, Isochlorogenic acid A and Isochlorogenic acid C were identified by reference standard and the content were determined by UPLC. UPLC (Fig. 2) exerted a good specificity between the mixed calibration solution and the sample solution. The results of the calibration curve (Supplement Table 1) also exhibited a good linearity with correlation coefficient (R^2) more than 0.999 and a wide concentration range. The precision, stability, repeatability and recovery represented as RSD values (Supplement Table 2) were all less than 5.00%. All of the methodological validation results suggested that this method was accurate, reliable, sensitive, and considered suitable for accurately measuring the main compounds' content in ET. The content of ST, chlorogenic acid, isochlorogenic acid B, isochlorogenic acid A, and isochlorogenic acid C in ET was measured as 0.426% 0.457% 0.159% 0.701%, and 0.103% respectively.

3.3 Screening of the Active compounds

A total of 15 compounds showed high pharmacokinetic properties and drug likeness in SwissADME or OB ≥ 30% and DL ≥ 0.18 in TCMSP. These components were selected as the active components of ET. The detailed information of 15 active compounds was listed in Table 3.

Table 3
15 active compounds of ET

NO.	Name	NO.	Name
1	Tricin	9	Diosmetin
2	ST	10	Esculetin
3	Quercetin	11	L-Malic
4	molephantinin	12	Maleic acid
5	Luteolin	13	Protocatechuic Aldehyde
6	Isodeoxyelephantopin	14	Protocatechuic acid
7	elephantopin	15	7-Hydroxycoumarine
8	Apigenin		

3.4 Compounds-targets Network and PPI-network Analysis

Compounds-targets Network and PPI-network Analysis were carried out to enrich the nuclear ingredients and nuclear targets. In this study, a total of 532 targets of the active ingredients were collected from TCMSP, HIT, and Swiss Target Prediction databases. Meanwhile, 19091 target of liver cancer from GeneCards, DisGenet, and OMIM databases were obtained by searching with the key word “Liver cancer”. Then, 520 overlapping targets (Supplementary Tables 3) of compound targets liver cancer related targets were analyzed by screened by Vene analysis (Fig. 3A) and the overlapping targets were regarded as hub targets. Compounds-targets Network was established (Fig. 3B). 7 nuclear compounds, including Quercetin, ST, Luteolin, Isodeoxyelephantopin, 7-Hydroxycoumarine, Elephantopin, and Esculetin were obtained by analyzing the top 10 parameter of Betweenness, Closeness, Information, and Degree (Fig. 3C). Meanwhile, 520 overlapping targets were submitted to STRING to conduct PPI-network (Fig. 3D). AKT1, TP53, TNF, IL6, ALB, SRC, EGFR, IL1B, BCL2, and CASP3 were the top 10 nuclear genes (Fig. 3E) based on the parameter of degree.

3.5 GO and KEGG Pathway Enrichment

GO and KEGG pathway enrichment analysis of the overlapping targets was carried out using Metascape. GO enrichment analysis suggested that a total of 166 molecular function (MF) terms (Supplementary Table 4), 1033 biological process (BP) terms (Supplementary Table 5), and 106 cellular component (CC) terms (Supplementary Table 6) were obtained. The GO functions related to the treatment of liver cancer included execution phase of apoptosis (GO:0097194), regulation of reactive oxygen species biosynthetic process (GO:1903426), oxidoreductase activity (GO:0016491), positive regulation of programmed cell death (GO:0043068), positive regulation of programmed cell death (GO:0043068), negative regulation of cell population proliferation (GO:0008285), response to oxygen levels (GO:0070482), response to decreased oxygen levels (GO:0036293), cellular response to oxygen levels (GO:0071453), cellular response to decreased oxygen levels (GO:0036294), mostly related to promote apoptosis, inhibit proliferation, and regulate oxidative levels. The top 20 entries were respectively selected from MF, BP, and CC, in order of -lg p value (Fig. 4A-C).

KEGG analysis explored 188 signaling pathways (Supplementary Tables 7) related to the 520 overlapping targets. The top 50 entries were selected depending on the -lg p value and showed in Fig. 4D. Among them, pathway in cancer (hsa05200) was significantly enriched in top 1, indicating the potential for anti-cancer activity of ET. Meanwhile, promoting apoptosis and inhibiting proliferation related signaling pathways, such as p53 signaling pathway (hsa04115) and MAPK signaling pathway (hsa04010) also collected.

3.6 Molecular Docking results

According to the result of quantitative analysis, ST is one of the main chemical compounds of ET. Moreover, ST is a nuclear compound in anti-liver cancer network pharmacology analysis of ET, which has been reported to show anti-cancer effect in vitro [11,12]. Therefore, ST was chose for further anti-cancer mechanical study. TGFBR1 is a membrane receptor for TGF-β1. Coincidentally, the activity of TGFBR1 is closely related to p38 MAPK/P53 signaling pathway. To further explored the relationship between the nuclear compounds and p38 MAPK/P53 signaling pathway. Molecular docking was used to present the binding affinities of ST and TGFBR1. The result was showed that ST had good binding affinities to TGFBR1, with the binding affinity energy as -9.3 kcal/mol, suggesting ST may mediate p38 MAPK/P53 signaling pathway by binding to TGFBR1.

3.7 ST promote the apoptosis of HepG2

The anti-liver cancer effect on HepG2 was validated in this study. The date revealed that ST at a concentration of 10 μM significantly caused changes in cell morphology (Fig. 5). CCK-8 result also indicated that ST notably inhibited the cell viability of HepG2 when compared with control group (Fig. 5F) and the concentration of 5 μM was chose for further mechanical study in HepG2. Cell morphology changing and cell viability decreasing indicated that ST showed anti-liver cancer effect by inducing cell apoptosis.

(0 μM). (B) Cell morphology in 1.25 μM. (C) Cell morphology in 2.50 μM. (D) Cell morphology in 5.00 μM. (E) Cell morphology in 10.00 μM. (F) Cell viability of different doses of ET after treatment for 24. Data are shown as mean ± standard deviation from three independent experiments. *$p < 0.05$ versus the control.

3.8 ST regulated apoptosis related nuclear genes' expression in mRNA level

Previous study indicated that abnormal expression of CASP3 [13], TNF-α [14], IL6 [15], IL1β [16], BCL2 [17], and TP53 [18] in mRNA level closely related to the proliferation or apoptosis of cancer cells. Quantitative Real-Time PCR result reveal that ST downregulated BCL2, IL6, TNF-α, IL1β, and EGFR while upregulated CASP3 and TP53 in mRNA level when compared with control group (Fig. 6).

3.9 ST promote apoptosis of HepG2 via p38 MAPK/p53 signaling pathway

Core proteins of p38 MAPK/p53 signaling pathway in HepG2 were detected by western blotting (Fig. 7). The result indicated that ST notably promoted the protein expression level of p-p38/p38 ($p < 0.05$) and p-p53/p53 ($p < 0.05$), indicating ST significantly active p38 MAPK/p53 signaling pathway in HepG2. Meanwhile, BCL-2 and CASP3, core targets of network pharmacology, closely related to cell apoptosis were inhibited and promoted respectively, indicating ST promote apoptosis of HepG2.

Discussion

Liver cancer is the fourth leading cause of cancer death all over the world [19]. Nowadays, surgical interventions are regarded as the most effective approach for liver cancer. However, extrahepatic metastasis only suitable for limited patients [20]. Meanwhile, current liver cancer drugs, such as Sorafenib, usually exert limited effects but bring with many side effects and hepatotoxicity [21]. Therefore, excavating alternative treatment for liver cancer is still urgent needed.

Natural compounds may exert better outcomes in anti-cancer [1]. Moreover, taking traditional herb medicine with anti-cancer effect natural compounds show fewer side effects and lower systemic toxicity [22]. ET have long been used as a folk traditional medicine in south of China [6]. Sesquiterpene lactones from ET show significant anti-cancer activity [6]. Herein, UPLC-Q-TOF-MS/MS qualitative analysis, UPLC quantitative analysis and network pharmacology analysis by combining ET and liver-cancer were used to predict the anti-liver cancer ingredients in ET. The result indicated that ST, a sesquiterpene lactone compound, is a nuclear compound in anti-liver cancer. Anti-liver cancer effect of ST was validated on HepG2 and ST significantly inhibited the proliferation of HepG2 in a concentration of 10 μM. Molecule docking, RT-qPCR, and western blotting were applied to explore the anti-liver cancer potential mechanism of ST. Molecule docking result indicated that ST showed a stable binding with TGFBR1, which is a cell

membrane receptor and a key upstream protein of p38MAPK signaling pathway. RT-qPCR experiment also confirmed that TP53, the tumour suppressor gene [18][36859359] and the core downstream gene of p38MAPK signaling pathway, was notably upregulated by ST treatment in HepG2, indicating that ST may bind to TGFBR1 and activate p38MAPK/p53 signaling pathway, which medicate proliferation and apoptosis [23,24].

BCL-2 is an anti-apoptotic gene, which forms heterodimers with BAX. The BAX/BCL-2 ratio plays a role in the balance of apoptosis [25]. BAX is an important TP53 target [26]. Activating TP53 may in turn increases BAX protein expression, activates CASP3 protein expression and subsequently induces apoptosis [27]. In this study, we carried out in vitro experiment to demonstrate that ST promote apoptosis by upregulate TP53, CASP3 and downregulate BCL2 in mRNA and protein expression level, suggesting ST may induce apoptosis of HepG2 by activating TP53/CASP3 signaling pathway.

Inflammation has been proved to associate with the development of cancer and modulating the inflammatory microenvironment provide an efficient therapy for cancer [28]. IL-1β, IL-6, and TNF-α are the crucial inflammatory cytokines and have been proved to influence the progression liver cancer [29–31]. In this study, nuclear genes related to IL-1β, IL-6, and TNF-α were all be enriched via network pharmacology analysis. Furthermore, in vitro experiment indicated that the nuclear compound ST inhibited the mRNA expression level of IL-1β, IL-6, and TNF-α, verifying the prediction of network pharmacology analysis and giving a sign into the anti-liver cancer effect of ST.

We previous suggested that ST showed a significantly inhibition on A549 [11], and the anti-cancer effect of ST was also validated on bladder cancer cell [32]. In this study, we firstly validated the anti-cancer effect of ST on HepG2 and elucidated the potential mechanism. ST, the second main compound of ET, can be regarded as Q-marker of ET, deserving deep study on efficacy and mechanism in vivo and providing anti-liver cancer an alternative treatment.

Conclusion

In summary, we first explored the chemical composition using UPLC-Q-TOF-MS/MS and 42 compounds were identified. Among the compounds being identified, ST, chlorogenic acid, Isochlorogenic acid B, Isochlorogenic acid A and Isochlorogenic acid C were the main compounds. Network pharmacology analysis suggested that ST is the core anti-liver cancer compound and the effect of ST in inhibiting HepG2 proliferation was first validated. Molecule docking date indicated that ST have a stable bind to TGFBR1, which is the upstream protein of p38MAPK signaling pathway. In vitro experiment on HepG2 demonstrated that ST promoted apoptosis by p38MAPK/p53 signaling pathway (Fig. 8). ST can be regarded as Q-marker of ET in the field of anti-cancer.

Abbreviations

ET *Elephantopus tomentosus* Linn.

BCL-2 B-cell lymphoma-2

CASP3 Caspase-3

ESI Electrospray ionization

GO Gene Ontology

IDA Information-dependent acquisition

KEGG Kyto Encyclopedia of Genes and Genomes

MS Mass spectrometry

PPI protein-protein interaction

Q-TOF Quadrupole-Time of Flight

RT-qPCR Real-time quantitative polymerase chain reaction

Scabertopin (ST)

TCM Traditional Chinese medicine

TIC Total ion chromatography

UPLC Ultra performance liquid chromatography

Declarations

AUTHOR CONTRIBUTIONS

Canchao Jia carried out most of the *in vitro* experiments and wrote the original draft. Zhihao Zeng, Guanlin Xiao screened for active compound via Network pharmacology and molecular docking. LI Lingjie, JIA Dezheng, TANG Ruiyin[1], LI Yangxue, and JIANG Jieyi assisted in compounds analysis or in vitro experiments. Dake Cai, designed and supervised all the studies, and reviewed the manuscript. Xiaoli Bi, funding acquisition, designed and supervised all the studies.

FUNDING

This study was supported by the Scientific Research Project of Traditional Chinese Medicine Bureau of Guangdong Province, China (Grant No. 20222016 and 20212120); Guangdong Provincial Department of Science and Technology, China (Grant No. 2022A1515220171).

The permissions statement of collecting *Elephantopus tomentosus* Linn.

Elephantopus tomentosus Linn. is not a specie at risk of extinctio, which widely grow in southern China. *Elephantopus tomentosus* Linn. in this study was planted in Medicinal Botanical Garden of Guangzhou University of Chinese Medicine (Guangzhou, China) and was allowed to collect by Zhan Lu, who is the administrator of the Medicinal Botanical Garden of Guangzhou University of Chinese Medicine. All the collection of *Elephantopus tomentosus* Linn. comply with relevant institutional, national, and international guidelines and legislation of Convention on the Trade in Endangered Species of Wild Fauna and Flora and IUCN Policy Statement on Research Involving Species at Risk of Extinctio.

Data Availability

All data generated or analysed during this study are included in this published article and are available from the corresponding author on reasonable request.

References

1. Anwanwan, D., Singh, S.K., Singh, S., Saikam, V. & Singh, R. Challenges in liver cancer and possible treatment approaches. *Biochimica et Biophysica Acta (BBA) - Reviews on Cancer* **1873**(2020).
2. Marengo, A., Rosso, C. & Bugianesi, E. Liver Cancer: Connections with Obesity, Fatty Liver, and Cirrhosis. *Annual Review of Medicine* **67**, 103-117 (2016).
3. Singh, A.K., Kumar, R. & Pandey, A.K. Hepatocellular Carcinoma: Causes, Mechanism of Progression and Biomarkers. *Current Chemical Genomics and Translational Medicine* **12**, 9-26 (2018).
4. Liu, Y.*, et al.* Cellular senescence and cancer: Focusing on traditional Chinese medicine and natural products. *Cell Proliferation* **53**(2020).
5. Xiang, Y., Guo, Z., Zhu, P., Chen, J. & Huang, Y. Traditional Chinese medicine as a cancer treatment: Modern perspectives of ancient but advanced science. *Cancer Medicine* **8**, 1958-1975 (2019).
6. Guo, Z.K.*, et al.* Tomenphantadenine, an unprecedented germacranolide-adenine hybrid heterodimer from the medicinal plant Elephantopus tomentosus L. *Fitoterapia* **125**, 217-220 (2018).
7. Kurokawa, T.*, et al.* Deoxyelephantopin and its interrelation with elephantopin. *Tetrahedron Letters* **11**, 2863-2866 (1970).
8. Wang, B.*, et al.* A new sesquiterpene lactone fromElephantopus tomentosus. *Journal of Asian Natural Products Research* **14**, 700-703 (2012).
9. Bai, M.*, et al.* Highly Oxidized Germacranolides from Elephantopus tomentosus and the Configurational Revision of Some Previously Reported Analogues. *Journal of Natural Products* **85**, 2433-2444 (2022).
10. Shannon, P.*, et al.* Cytoscape: A Software Environment for Integrated Models of Biomolecular Interaction Networks. *Genome Research* **13**, 2498-2504 (2003).
11. Can-Chao Jia, L.-J.L., Zhi-Hao Zeng, Rui-Yin Tang, De-Zheng Jia, Min-Juan Yang, Jin-Yan Qiu, Dong-Mei Li, Can-Hui Xie, Guang-Ying Wu, Yang-Xue Li, Jie-Yi Jiang, Hong Huang, Guan-Lin Xiao, Da-Ke Cai, Xiao-Li Bi Prediction and analysis of Q-markers of Elephantopus scaber based on its UPLC

fingerprint, content determination of components, and in vitro a nti-tumor activity. *Zhongguo Zhong Yao Za Zhi* **48(16)**, 4421-4428 (2023).

12. Xu G, L.Q., Gong Z, Yu W, He S, Xi L. Antitumor activities of the four sesquiterpene lactones from Elephantopus scaber L. *Exp Oncol* **28(2)**(2006).
13. Ke, H.*, et al.* Effect of weimaining on apoptosis and Caspase-3 expression in a breast cancer mouse model. *Journal of Ethnopharmacology* **264**(2021).
14. Cruceriu, D., Baldasici, O., Balacescu, O. & Berindan-Neagoe, I. The dual role of tumor necrosis factor-alpha (TNF-α) in breast cancer: molecular insights and therapeutic approaches. *Cellular Oncology* **43**, 1-18 (2020).
15. Kumari, N., Dwarakanath, B.S., Das, A. & Bhatt, A.N. Role of interleukin-6 in cancer progression and therapeutic resistance. *Tumor Biology* **37**, 11553-11572 (2016).
16. Malik, A. & Kanneganti, T.D. Function and regulation of IL-1α in inflammatory diseases and cancer. *Immunological Reviews* **281**, 124-137 (2017).
17. Zhang, Y., Yang, X., Ge, X. & Zhang, F. Puerarin attenuates neurological deficits via Bcl-2/Bax/cleaved caspase-3 and Sirt3/SOD2 apoptotic pathways in subarachnoid hemorrhage mice. *Biomedicine & Pharmacotherapy* **109**, 726-733 (2019).
18. Wang, H., Guo, M., Wei, H. & Chen, Y. Targeting p53 pathways: mechanisms, structures, and advances in therapy. *Signal Transduction and Targeted Therapy* **8**(2023).
19. Liao, X., Bu, Y. & Jia, Q. Traditional Chinese medicine as supportive care for the management of liver cancer: Past, present, and future. *Genes & Diseases* **7**, 370-379 (2020).
20. Zhou, Y.*, et al.* Dietary Natural Products for Prevention and Treatment of Liver Cancer. *Nutrients* **8**(2016).
21. Chen, J.*, et al.* Potential molecular, cellular and microenvironmental mechanism of sorafenib resistance in hepatocellular carcinoma. *Cancer Letters* **367**, 1-11 (2015).
22. Zhang, X., Qiu, H., Li, C., Cai, P. & Qi, F. The positive role of traditional Chinese medicine as an adjunctive therapy for cancer. *BioScience Trends* **15**, 283-298 (2021).
23. Hsieh, T.C., Wong, C., John Bennett, D. & Wu, J.M. Regulation of p53 and cell proliferation by resveratrol and its derivatives in breast cancer cells: An in silico and biochemical approach targeting integrin αvβ3. *International Journal of Cancer* **129**, 2732-2743 (2011).
24. Wu, G.S. The functional Interactions Between the MAPK and p53 Signaling Pathways. *Cancer Biology & Therapy* **3**, 156-161 (2014).
25. Cahyadi, A.*, et al.* Relationship between Bax and Bcl-2 Protein Expression and Outcome of Induction Phase Chemotherapy in Pediatric Acute Lymphoblastic Leukemia. *Asian Pacific Journal of Cancer Prevention* **23**, 1679-1685 (2022).
26. Huang, C.-l., Yokomise, H. & Miyatake, A. Clinical significance of the p53 pathway and associated gene therapy in non-small cell lung cancers. *Future Oncology* **3**, 83-93 (2007).

27. Zhang, G.*, et al.* Dioscin suppresses hepatocellular carcinoma tumor growth by inducing apoptosis and regulation of TP53, BAX, BCL2 and cleaved CASP3. *Phytomedicine* **23**, 1329-1336 (2016).
28. Lan, T., Chen, L. & Wei, X. Inflammatory Cytokines in Cancer: Comprehensive Understanding and Clinical Progress in Gene Therapy. *Cells* **10**(2021).
29. Tiegs, G. & Horst, A.K. TNF in the liver: targeting a central player in inflammation. *Seminars in Immunopathology* **44**, 445-459 (2022).
30. Li, H.*, et al.* Long noncoding RNA lncGALM increases risk of liver metastasis in gallbladder cancer through facilitating N-cadherin and IL-1β-dependent liver arrest and tumor extravasation. *Clinical and Translational Medicine* **10**(2020).
31. Schmidt-Arras, D. & Rose-John, S. IL-6 pathway in the liver: From physiopathology to therapy. *Journal of Hepatology* **64**, 1403-1415 (2016).
32. Gao, Y.*, et al.* ST Derived from Elephantopus scaber L. Mediates Necroptosis by Inducing Reactive Oxygen Species Production in Bladder Cancer In Vitro. *Cancers* **14**(2022).

Figures

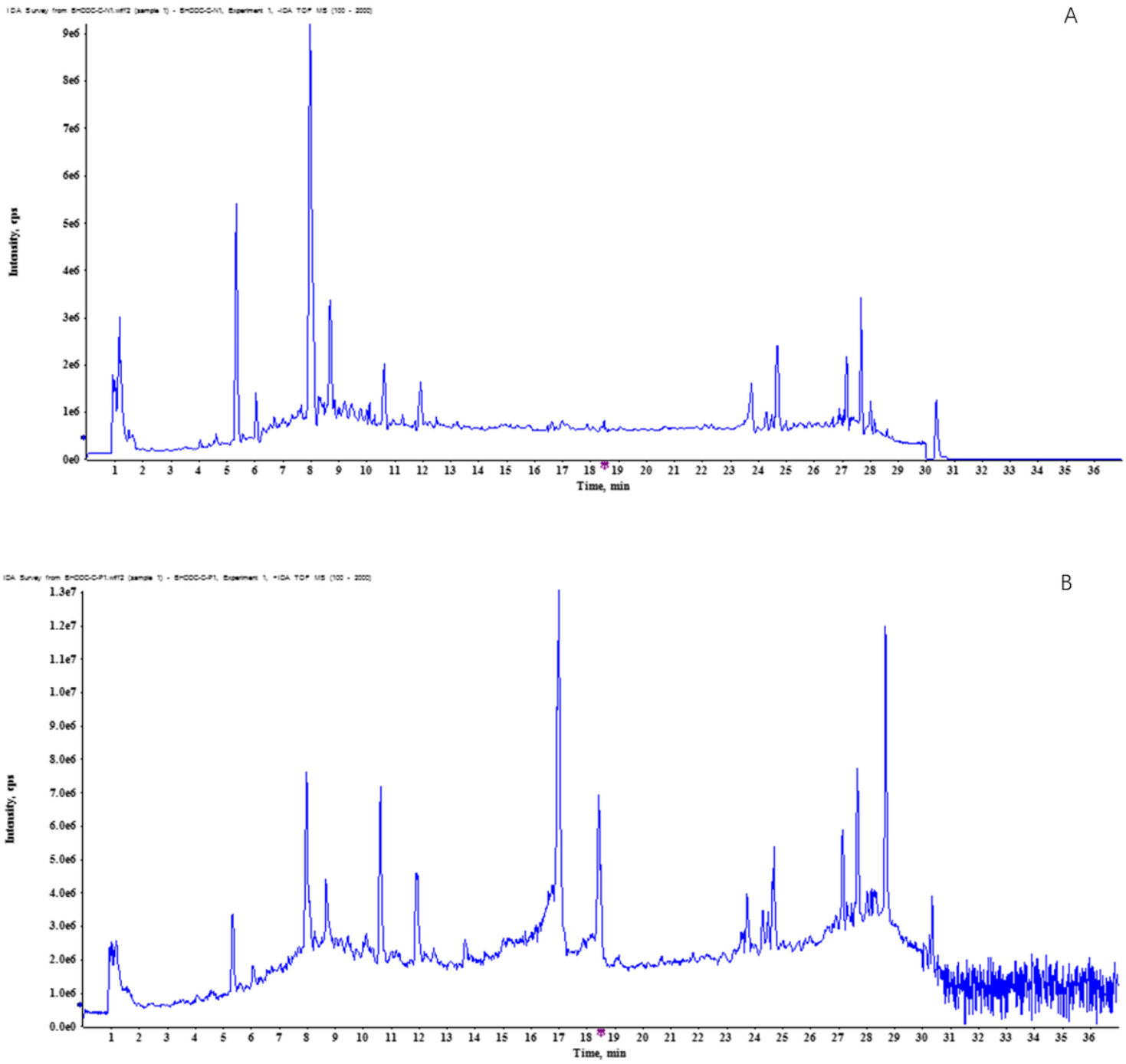

Figure 1

The total ion chromatography (TIC) of ET in positive(A) and negative (B) ion modes

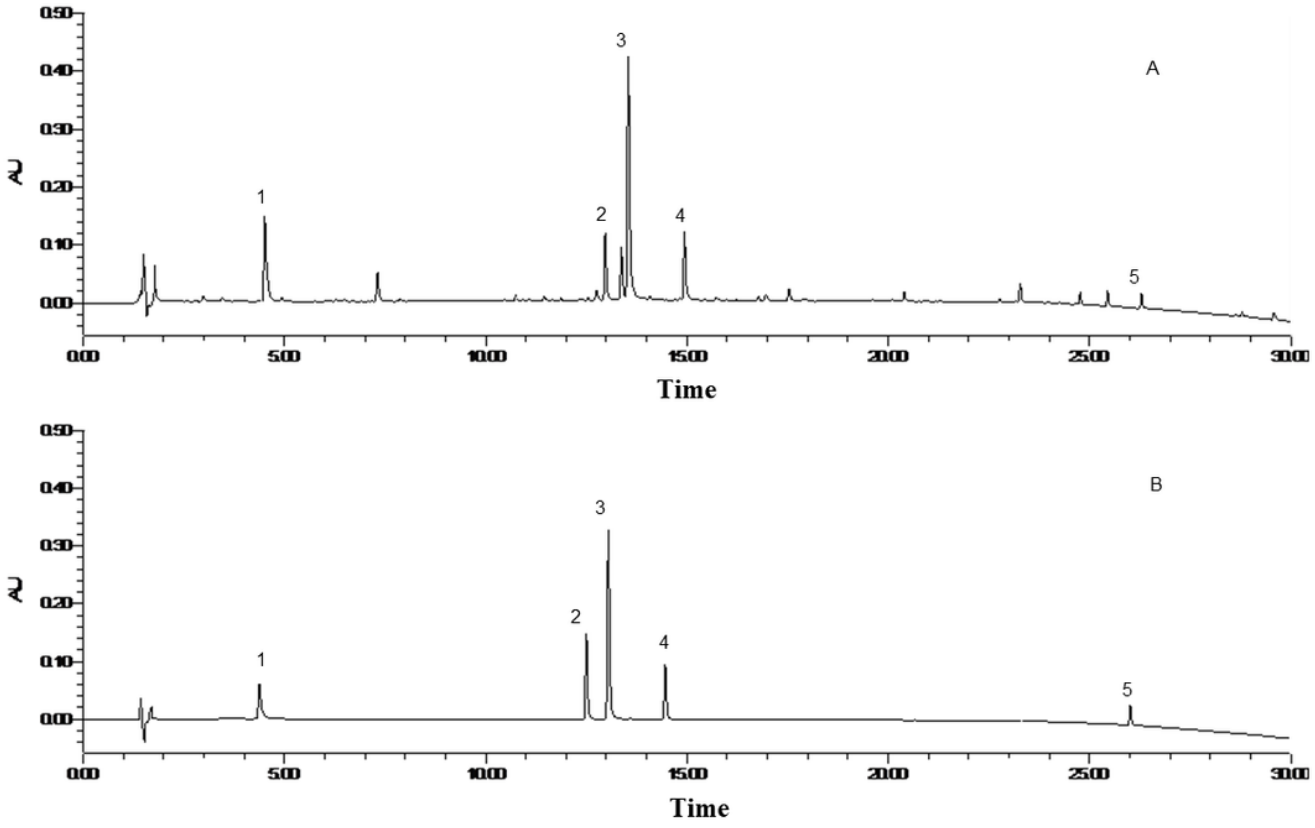

Figure 2

UPLC of ET sample solution (A) and standard solution (B). 1 Chlorogenic acid. 2 Sochlorogenic acid B. 3 Sochlorogenic acid A. 4 Sochlorogenic acid C. 5 ST.

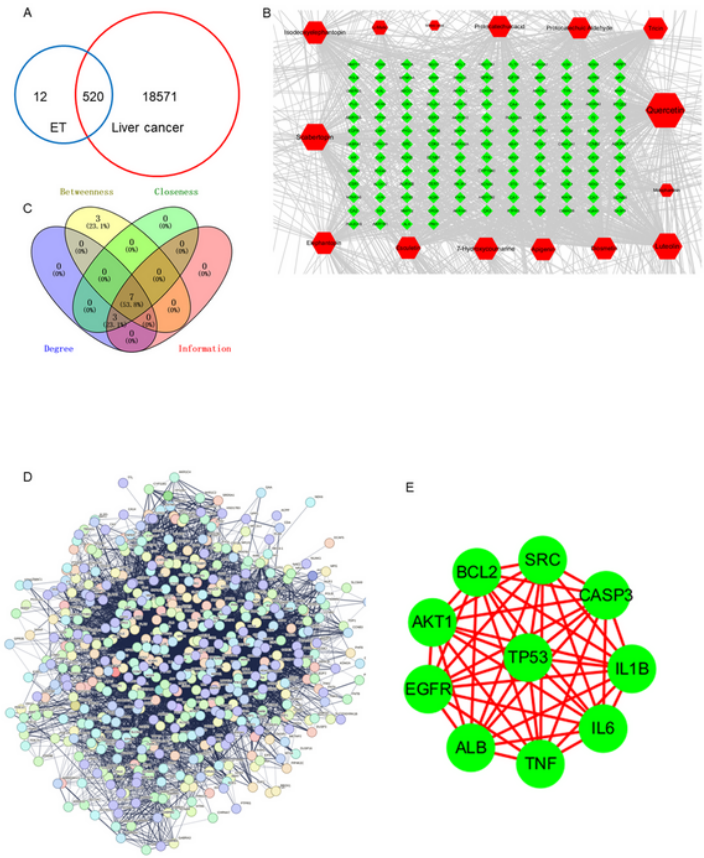

Figure 3

Network pharmacology analysis. (A) Overlapping targets collected by vene analysis. (B) Compounds-targets Network. (C) Nuclear compounds enrichment. (D) PPI-network. (E) Nuclear targets enrichment.

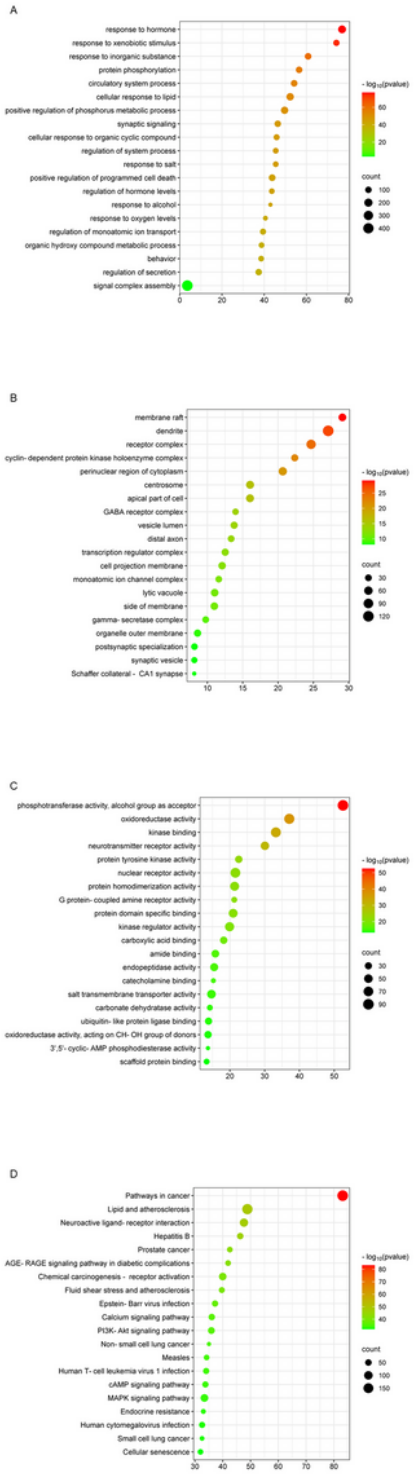

Figure 4

GO and KEGG enrichment. (A) MF enrichment. (B) BP enrichment. (C) CC enrichment. (D) KEGG enrichment.

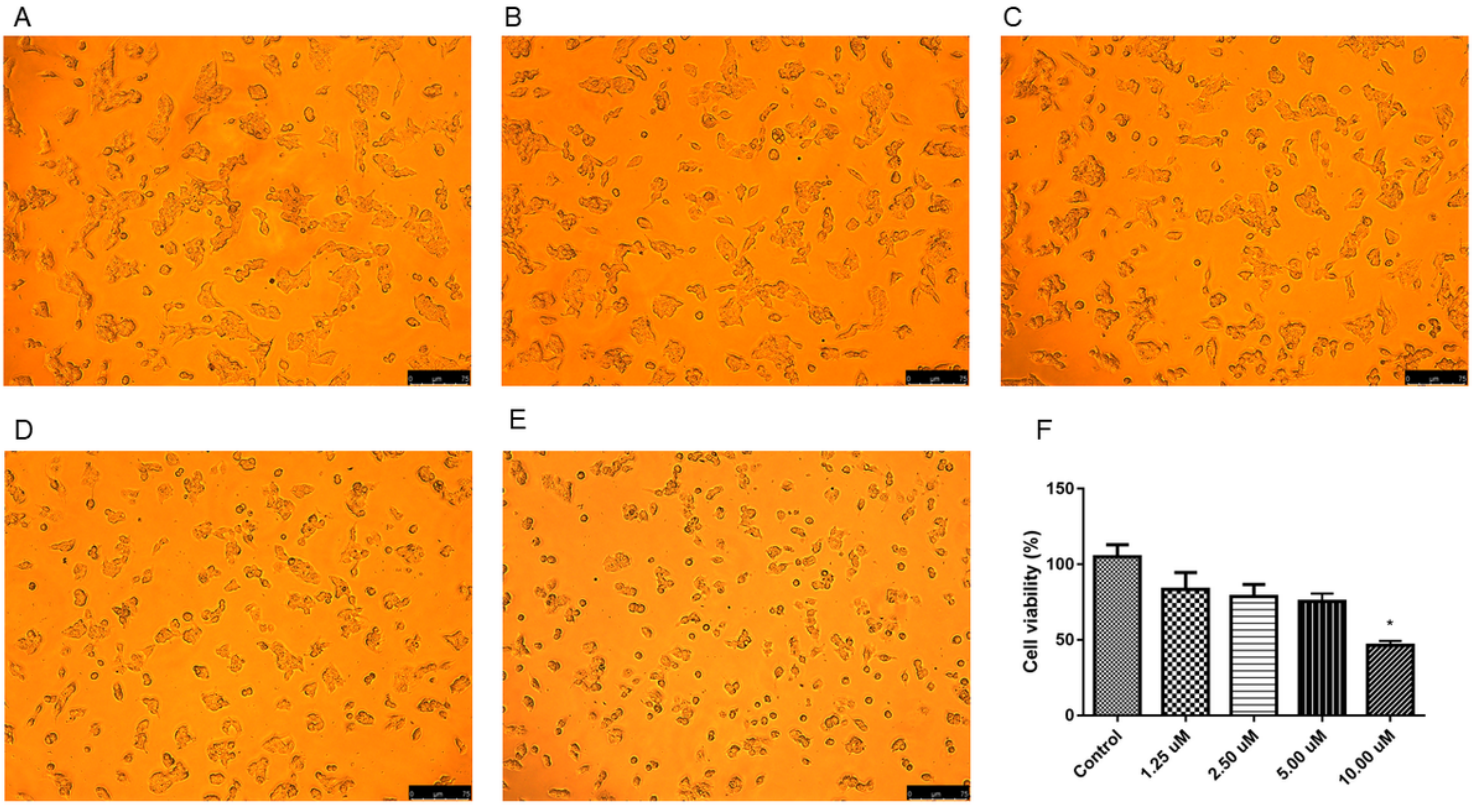

Figure 5

ST inhibited the proliferation of HepG2. (A) Cell morphology in control group

(0 μM). (B) Cell morphology in 1.25 μM. (C) Cell morphology in 2.50 μM. (D) Cell morphology in 5.00 μM. (E) Cell morphology in 10.00 μM. (F) Cell viability of different doses of ET after treatment for 24. Data are shown as mean ± standard deviation from three independent experiments. *p < 0.05 versus the control.

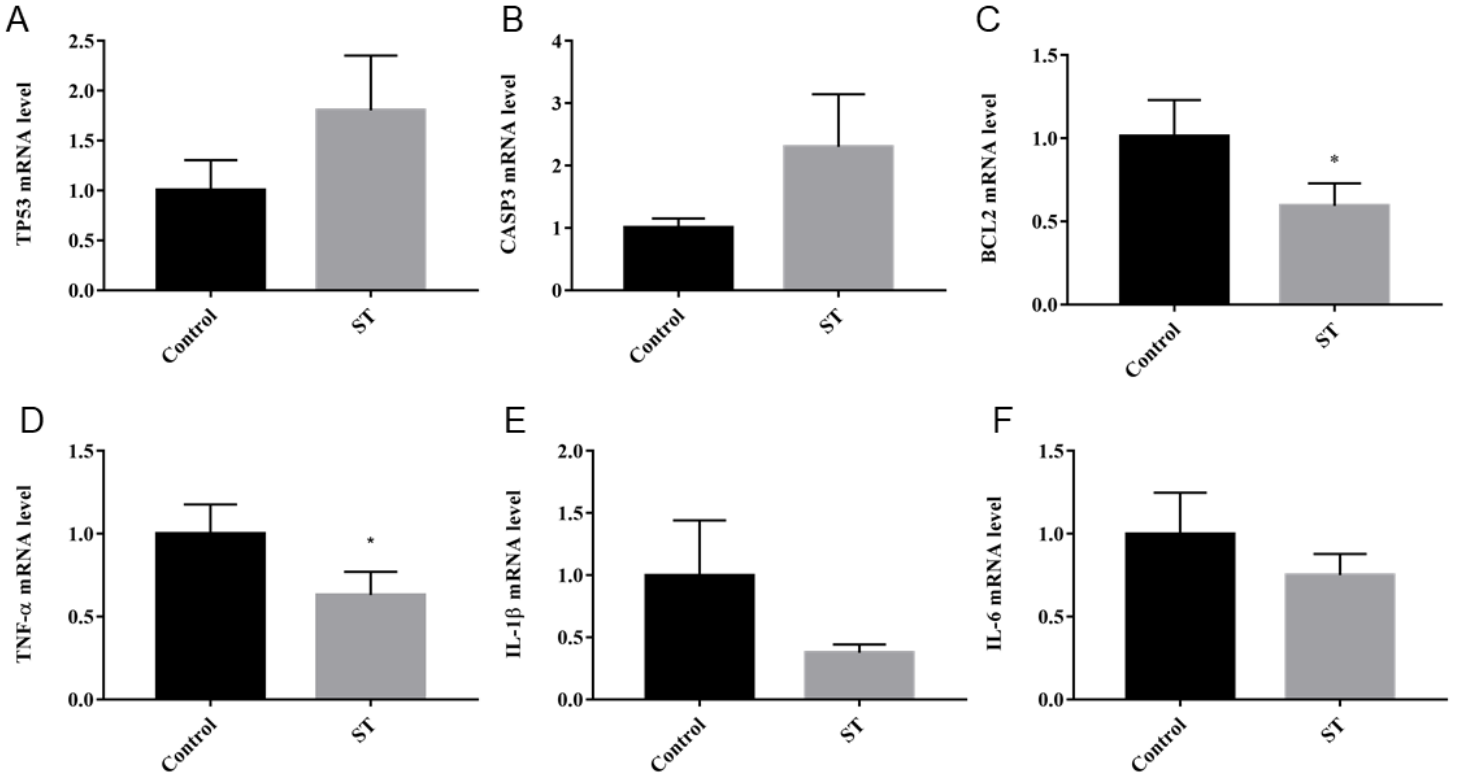

Figure 6

ST regulated apoptosis related nuclear genes' expression in mRNA level. (A) The mRNA levels of TP53. (B) The mRNA levels of CASP3. (C) The mRNA levels of BCL2. (D) The mRNA levels of TNF-α. (E) The mRNA levels of IL-1β. (F) The mRNA levels of IL-6. GAPDH was used for normalization. *p < 0.05 versus the control.

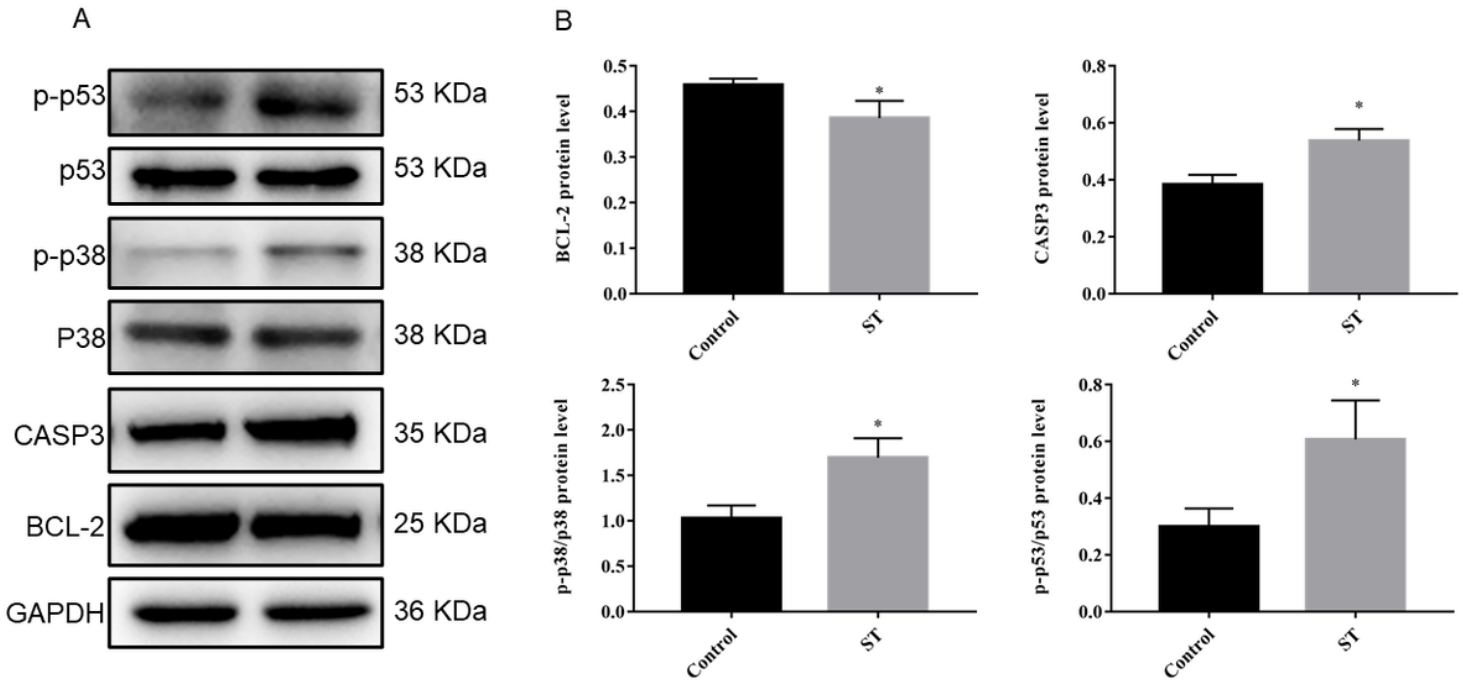

Figure 7

ST promote apoptosis of HepG2 via p38 MAPK/p53 signaling pathway. (A) The protein levels of p-p53, p53, p-p38, p38, CASP3, and BCL-2 in HepG2 cells treated with ST for 24 h were determined by Western blot analysis. (B) Quantitative analysis of BCL-2, CASP3, p-p38/p38, and p-p53/p53. GAPDH was used as the loading control. *p < 0.05 versus the control.

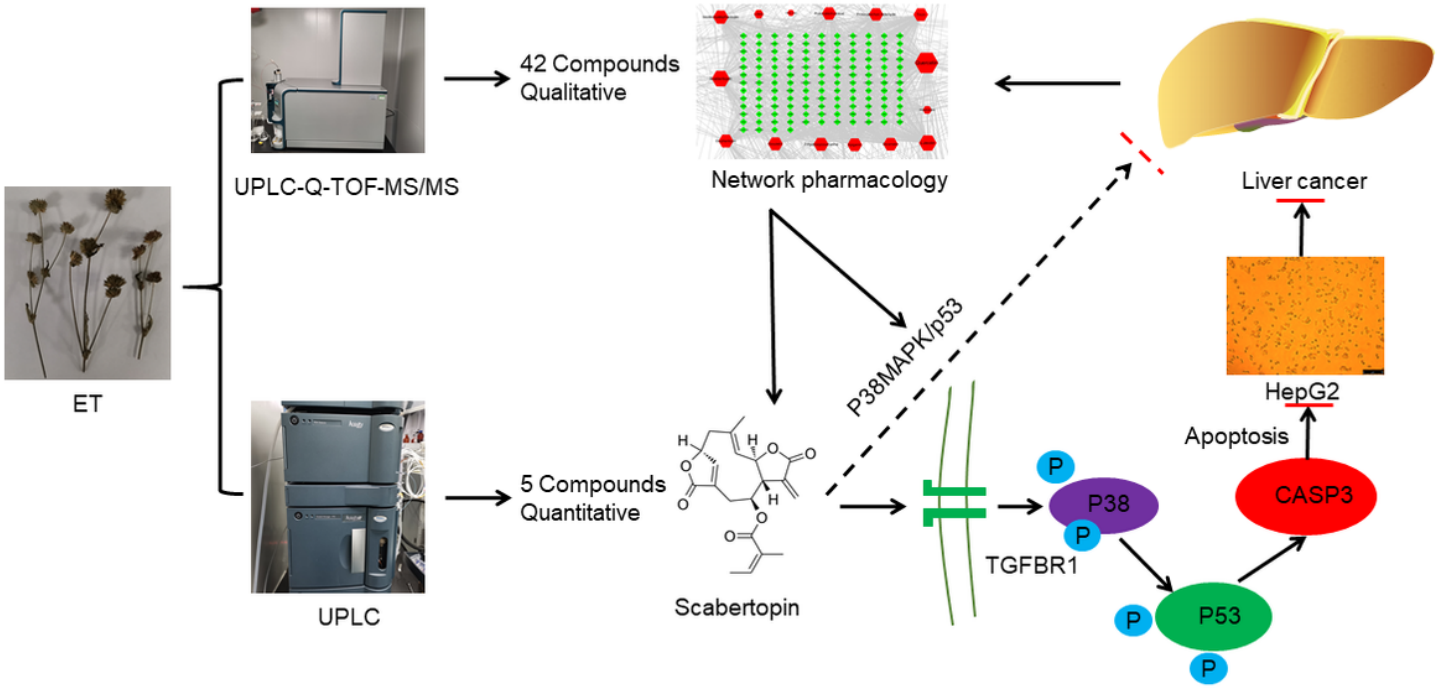

Figure 8

ST, an anti-liver tumor ingredient of *Elephantopus tomentosus*Linn., promote apoptosis of HepG2 via p38 MAPK/p53 signaling pathway

Supplementary Files

This is a list of supplementary files associated with this preprint. Click to download.

- Supplementtable20240102.pdf
- Rawdata20240102.pdf